

Numerical simulation on single bubble behavior during Al₂O₃/H₂O nanofluids flow boiling using Moving Particle Semi-implicit method



Yun Wang, Jun Mei Wu*

State Key Laboratory for Strength and Vibration of Mechanical Structures, School of Nuclear Science and Technology, Xi'an Jiaotong University, Xianning West Road 28#, Xi'an 710049, China

ARTICLE INFO

Article history:

Received 10 April 2015

Received in revised form

6 June 2015

Accepted 12 June 2015

Available online 23 June 2015

Keywords:

Al₂O₃/H₂O nanofluids

Flow boiling

Bubble behavior

MPS

ABSTRACT

In this study, regression analysis on the thermal properties of Al₂O₃/H₂O nanofluids was made firstly. The growth and departure of a single bubble behavior in Al₂O₃/H₂O nanofluid and pure water flow boiling process were then numerically simulated by an improved Moving Particle Semi-implicit method in different flow boiling conditions. The results indicate that the bubble in Al₂O₃/H₂O nanofluids grows faster and the bubble departure frequency of Al₂O₃/H₂O nanofluids is greater than that in pure water. The flow boiling heat flux is also improved by dispersing nanoparticles of Al₂O₃/H₂O in pure water. This work initially reveals that nanofluids can enhance flow boiling heat transfer from the point of view of bubble dynamics behavior. The effects of nanoparticle concentrations and diameters of Al₂O₃/H₂O nanofluids on the bubble behavior were also investigated and compared under the same flow conditions. It is found that the increasing of nanoparticle volume concentration may increase the bubble departure frequency and departure diameter, while the increasing rates of departure frequency and departure diameter are lessened with the increasing of nanoparticle volume concentration. It is suggested that the suitable nanoparticle volume concentration of nanofluid for flow boiling heat transfer enhancement should not be too large, especially regarding the negative effect of flow resistance increase due to the increasing of nanoparticle volume concentration. The interesting finding is that in the same nanoparticle volume concentration condition, the bubble departure frequency for the nanofluid with nanoparticle diameter of 29 nm shows a maximum value. The increasing of nanoparticle diameter leads to the decreasing of bubble departure diameter. It is boldly to predict that an optimal nanoparticle diameter range between 20 and 38 nm should be beneficial to flow boiling heat transfer enhancement of Al₂O₃/H₂O nanofluids.

© 2015 Elsevier Ltd. All rights reserved.

1. Introduction

Compared with conventional heat transfer working fluid, nanofluids dispersed with suitable nano-scale metallic or nonmetallic particles can bring significant increasing of thermal conductivity. The potential applications of nanofluids in many high heat flux thermal management systems have attracted numerous research interests worldwide. The researches on nanofluids convective heat transfer, boiling heat transfer and critical heat flux are increasing exponentially every year. Nanofluids as a novel

strategy to improve heat transfer characteristics of fluids by the addition of solid particles with diameters below 100 nm were proposed by Choi (1995) early in the 1990s. Very small amount of guest nanoparticles were found to provide dramatic improvements in thermal properties of base fluids. A nonlinear relationship exists between nanofluid's thermal conductivity and its concentration and temperature. Nanofluids are thus being considered as innovative and potential working fluids for heat transfer enhancement. Since You et al. (2003) first reported that the CHF of Al₂O₃/H₂O nanofluids pool boiling with particle concentrations ranging from 0 g/l to 0.05 g/l was increased by approximately 200% compared with that of pure water, nanofluids have been expected to be ideally suited for practical thermal systems where high heat flux removal is needed, such as in nuclear reactors. Thus, the characteristics of nanofluids boiling heat transfer, especially the characteristics of critical boiling, have become a hot research topic worldwide. Das

* Corresponding author. School of Aerospace, Xi'an Jiaotong University, Xi'an City 710049, China.

E-mail address: wjmxjtu@mail.xjtu.edu.cn (J.M. Wu).

Nomenclature		δ	heat conductivity thickness (m)
A	Heat transfer area (m ²)	φ	slant angle (°)
c_p	specific heat at constant pressure (kJ/kg K)	θ	angle (°)
d	diameter (m)	<i>Superscripts</i>	
h_{fg}	latent heat (J/kg)	0	standard temperature of 293.15 K
k	thermal conductivity (W/m k)	Bi	bubble interior
k_B	Boltzmann constant	f	base fluid
M	relative molecular weight	$f0$	standard state of atmospheric pressure and 273.15 K in temperature
N	Avogadro constant	fr	standard of freezing point
Pr	Prandtl number	g	gas phase
Q	heat (J)	i	particle number
Re	Reynolds number	l	liquid phase
T	Temperature (K)	nf	nanofluids
Δt	time step (s)	p	particle
<i>Greek symbols</i>		w	heating surface
ρ	density of nanofluid (kg/m ³)	<i>Abbreviations</i>	
ν	dynamic viscosity (kg/m s)	MPS	Moving Particle Semi-implicit
σ	surface tension (N/m)	MAFL	Meshless Advection using Flow-directional Local-grid
κ	curvature (1/m)	CHF	critical heat flux
α	thermal diffusivity (m ² /s)		

et al., 2003a, 2003b) conducted research on Al₂O₃/H₂O nanofluids pool boiling at atmospheric pressure and found that within a given heat flux density, the wall superheat had been increased with the increasing of nanoparticle volume concentration. The result indicated that nanoparticles deteriorated the pool boiling heat transfer. And they suggested that the trapped nanoparticles changed the heating surface characteristics during boiling. Park et al. (2009) experimental results showed that the pool boiling heat transfer coefficients of the aqueous solutions with CNTs were lower than those of pure water in the entire nucleate boiling regime. While Taylor and Phelan (2009) reported some new but limited experimental data for Al₂O₃/H₂O nanofluids that indicated that nucleate boiling incipience occurred 2–3 °C earlier, and nucleate boiling heat transfer was enhanced by 25–40%, but sub-cooled boiling was deteriorated, compared with the pure-water baseline. In contrast, other literature reported pool boiling heat transfer enhancements by nanofluids. The boiling curves for nanofluids were found in Truong (2007) experimental results to shift to the left of that for water, corresponding to higher nucleate boiling heat transfer coefficients in the two phase regime. Heris (2011) experimentally investigated the boiling heat transfer of the CuO/ethylene glycol-water (60/40) nanofluid. The results indicated that a considerable boiling heat transfer enhancement has been achieved, specifically that the enhancement had increased with increasing nanoparticles concentration and reached 55% at a nanoparticles loading of 0.5 vol. %. It is found that the current literature shows mixed or discrepant experimental results about the characteristics of nanofluids pool boiling heat transfer. This indicates, so far, that we have not yet understood the underlying mechanisms influencing boiling heat transfer of nanofluids. For most potential applications of nanofluids, flow boiling should still be an important research topic. Kim et al. (2008) carried out vertical tube flow boiling experiments of nanofluids at atmospheric pressure, low subcooling, and relatively high mass flux to investigate the CHF characteristics. A significant CHF enhancement (up to 30%) has been achieved by alumina nanoparticles as little as 0.01 Vol. %. Kim et al. (2010) conducted experiments to evaluate the possibility of enhancing CHF in flow boiling using Al₂O₃/H₂O nanofluids as working fluids vertically

flowing upward in the tube under atmospheric pressure. It was verified that the dispersion stability of Al₂O₃/H₂O nanofluids during the CHF experiment was sufficient when the concentration of the nanofluids was in a range 0.001–0.5 vol. %. The CHFs of Al₂O₃/H₂O nanofluids were enhanced up to about 70%, in flow boiling for all experiment conditions. It was suggested that nanoparticles deposition on the heating surface contributed to CHF enhancement. Ahn et al. (2010) performed an experimental study on CHF enhancements of forced convective boiling of 0.01 vol. % Al₂O₃/H₂O nanofluids in a horizontal rectangular channel. The experimental results showed that, compared to that in pure water, the nanofluid flow boiling CHF was enhanced 24% and 40% with velocity of 1 m/s and 4 m/s, respectively. The heating surface was characterized before and after boiling tests, and nanoparticles deposition was observed during boiling. Kim et al. (2011) and Ahn and Kim (2012) concluded that the flow boiling CHF enhancement was caused by nanoparticles deposition on the channel inner surface.

Vafaei and Wen (2011) were the first to discuss the dual effects of nanoparticles in boiling heat transfer: (i) modification of the heating surface through nanoparticle deposition and (ii) modification of bubble dynamics by varying contact angles, departure bubble volume, and frequency. The second role may open a promising window for future nanofluid applications in micro-channel heat transfer, avoiding the high increasing in pressure drop arising from nanoparticle deposition. Xu and Xu (2012) investigated the flow boiling heat transfer with and without Al₂O₃ nanoparticles in a single micro-channel with a platinum film for bottom surface heating. The flow boiling of pure water displayed chaotic behavior due to random bubble coalescence and breakup over millisecond timescales at moderate heat fluxes. Nevertheless, the nanofluid (weight concentration of 0.2%, consisting of de-ionized water and 40 nm Al₂O₃ nanoparticles) was found to mitigate significantly the flow instability and nanoparticle deposition on the heating surface was not observed. Flow boiling of the nanofluids was always stable or quasi-stable with significantly reduced pressure drop and enhanced heat transfer. This is an interesting finding that deserves to be studied more deeply.

Actually, the flow boiling heat transfer is very complex. The flow boiling heat transfer of nanofluids is governed by the thermo-properties of fluids, the surface characteristics of the heating surface and the flow regime. The boiling process includes the bubble generation, growth, and departure from the wall, motion and amalgamation within the fluid. The flow pattern will change during flow boiling process due to the bubble fusion and the changing of the void fraction in flowing fluid. Any changing above can lead to the change of flow boiling heat transfer condition. The flow boiling heat transfer in nanofluids is more complex than that in the water. The nanoparticle in the boiling nanofluids will produce effects on bubble generation, growth and departure from the wall, as well as motion and amalgamation within the fluid. Surface characteristics of the wall are just one of many aspects affecting bubble generation, growth, and departure. The collective effect of nanoparticles suspended in base liquid not only influences bubble generation, growth and departure, but also influences bubbles' motion and amalgamation in the flowing fluid. Shear stresses and temperature gradients in the fluid may result in a non-uniform distribution of nanoparticles, which will in turn influence the vapor distribution and flow pattern. Therefore, the nanofluids flow boiling heat transfer coefficient and CHF may be very different from that of base fluids because of the collective effect of suspended nanoparticles. So far, the research of nanofluids boiling heat transfer is less and limited. No research about the nanofluids boiling heat transfer characteristics from the viewpoint of bubble behavior is reported.

Taking these into consideration, the present authors numerically simulated single bubble growth and departure during flow boiling of $\text{Al}_2\text{O}_3/\text{H}_2\text{O}$ nanofluids and pure water at atmospheric pressure using moving particle semi-implicit (MPS) method in different flow boiling conditions. The effects of nanoparticle concentrations and diameters of $\text{Al}_2\text{O}_3/\text{H}_2\text{O}$ nanofluid on the bubble behavior were investigated and compared under the same conditions.

2. Thermo-physical properties of $\text{Al}_2\text{O}_3/\text{H}_2\text{O}$ nanofluids

Regarding the multi-phase flow and heat transfer performance of thermal systems, the key thermo-physical properties of fluids include density, specific heat capacity, thermal conductivity, viscosity and surface tension. Thus, changes in the thermo-physical properties of nanofluids compared with base fluids need to be estimated first before bubble behavior is simulated in this paper. The density and specific heat capacity of nanofluids can be estimated according to the mixture model, which is applicable to conventional fluid-solid mixtures, shown in Eqs. (1) and (2). However, the changes in thermal conductivity, viscosity, and surface tension of nanofluids are complicated but most interestingly unprecedented.

$$\rho_{nf} = \rho_p \phi + \rho_f (1 - \phi) \quad (1)$$

$$c_{p,nf} = \frac{\rho_p c_{p,p} \phi + \rho_f c_{p,f} (1 - \phi)}{\rho_p \phi + \rho_f (1 - \phi)} \quad (2)$$

So far, there are many publications to present the enhanced thermal conductivity as well as increased viscosity of different nanofluids in different conditions compared with base fluid. The trends of the relationship between the thermal conductivity or viscosity of nanofluid and their influence factors (temperature, size and volume concentration of nanoparticles) have been widely studied experimentally and/or theoretically. However, the experimental data of nanofluids' thermal properties are insufficient and scattered; especially the description of the relationship between the

thermal conductivity, dynamic viscosity coefficient and nanoparticle size, temperature is still very inconsistent (Christianson et al., 2011). Some models and/or empirical correlations have been proposed to predict the thermal conductivity and viscosity of nanofluids with limited application ranges. In past years surface tension of nanofluids received much less attention even if it is a very important parameter in fluid boiling as well as other two-phase heat transfer phenomena. Thus, we should carefully select the suitable and reliable models of thermo-physical properties of $\text{Al}_2\text{O}_3/\text{H}_2\text{O}$ nanofluids before we carry out the present simulation work.

2.1. Thermal conductivity

Koo and Kleinstreuer (2004) proposed a theoretical model (referred to KK) of nanofluids thermal conductivity in the form of Eq. (3). This model took into account the effect of Brownian motion, temperature, mean diameter, volume fraction of nanoparticles, thermal conductivities of the base fluid and nanoparticles on nanofluid thermal conductivity at temperatures in the range of 300–325 K.

$$\frac{k_{nf}}{k_f} = \frac{k_p + 2k_f - 2\phi(k_f - k_p)}{k_p + 2k_f + \phi(k_f - k_p)} + 5 \times 10^4 \frac{\beta \phi \rho_f c_{pf}}{k_f} \sqrt{\frac{k_B T}{\rho_p d_p}} f(T, \phi) \quad (3)$$

Where k_B is Boltzmann constant, and its value is $1.38066 \times 10^{-23} \text{ J K}^{-1}$. For $\text{Al}_2\text{O}_3/\text{H}_2\text{O}$ nanofluid, β and $f(T, \phi)$ are calculated by Eqs. (4) and (5).

$$\beta = \frac{8.4407}{(100\phi)^{1.07304}} \quad (4)$$

$$f(T, \phi) = \left(2.8217 \times 10^{-2} \phi + 3.917 \times 10^{-3} \right) \left(\frac{T}{T_0} \right) + \left(-3.0669 \times 10^{-2} \phi - 3.91123 \times 10^{-3} \right) \quad (5)$$

Vajjha and Das (2009) developed new correlations of β and $f(T, \phi)$ of three nanofluids based on their experiment data as follows:

$$\beta = \frac{0.0017}{(100\phi)^{0.0841}} \quad (6)$$

$$f(T, \phi) = (-6.04\phi + 0.4705)T + (1722.3\phi - 134.63) \quad (7)$$

Recently, Corcione (2011) proposed an empirical correlation to predict the effective thermal conductivity of different nanofluids (with nanoparticle of Al_2O_3 , CuO , TiO_2 and Cu dispersed in water or EG) as Eq. (8) for both numerical simulation purposes and thermal design tasks, based on a high number of experimental data available in the literature.

$$\frac{k_{nf}}{k_f} = 1 + 4.4 \text{Re}^{0.4} \text{Pr}^{0.66} \left(\frac{T}{T_{fr}} \right)^{10} \left(\frac{k_p}{k_f} \right)^{0.03} \phi^{0.66} \quad (8)$$

Where, T_{fr} is the freezing point of the base liquid, and Re is defined as:

$$\text{Re} = \frac{\rho_f k_B T}{\pi \eta_f^2 d_p} \quad (9)$$

In order to select a more suitable model or correlation of the thermal conductivity of $\text{Al}_2\text{O}_3/\text{H}_2\text{O}$ nanofluid for the present simulation, the predicted thermal conductivities of $\text{Al}_2\text{O}_3/\text{H}_2\text{O}$

nanofluid and the experimental data from Das et al. (2003a, b) (nominal particle size is 38.4 nm) are compared, as shown in Fig. 1. It is found that Corcione's empirical correlation can predict the thermal conductivity of Al₂O₃/H₂O with the maximum deviation less than 3.87%. Thus, Corcione's empirical correlation is used in the present simulation.

2.2. Dynamic viscosity

The most classical formula to calculate the dynamic viscosity of solid–liquid suspension is Einstein equation (Einstein, 1956), but it only applies to the suspension which is composed of millimeter and micrometer scale solid particles and based fluid. Nguyen et al. (2007) measured the dynamic viscosity of Al₂O₃/H₂O nanofluid, and developed Eq. (10) by the regression analysis based on their experimental data for nanoparticle diameter of 36 nm. Williams et al. (2008) and Corcione (2011) also presented correlations of nanofluids dynamic viscosity as Eqs. (11) and (12).

$$\eta_{nf} = \eta_f(T) \left(1 + 0.025\phi + 0.015\phi^2 \right) \tag{10}$$

$$\eta_{nf} = \eta_f(T) \exp\left(\frac{4.91\phi}{0.2092 - \phi} \right) \tag{11}$$

$$\eta_{nf} = \eta_f(T) / \left[1 - 34.87 \left(d_p / d_f \right)^{-0.3} \phi^{1.03} \right] \tag{12}$$

In Eq. (12), d_f is calculated by Eq. (13). The influence of temperature to the dynamic viscosity of nanofluids is considered in the dynamic viscosity of base fluid. The correlation between dynamic viscosity of pure water and temperature is expressed as Eq. (14).

$$d_f = 0.1 \left(\frac{6M}{N\pi\rho_f0} \right)^{1/3} \tag{13}$$

$$\eta_f(T) = \exp\left(\frac{1.12646 - 0.039638T}{1 - 0.00729769T} \right) \times 1.005 \times 10^{-7} \tag{14}$$

To obtain the suitable model of dynamic viscosity of Al₂O₃/H₂O, comparison is made between the results predicted by the three models and the data of the experiment (Das et al., 2003a, 2003b), shown in Fig. 2. It is found that the predicted result of Corcione model is most consistent with the experiment data with deviation less than 1.03%. Thus, Corcione's correlation is chosen to calculate dynamic viscosity of Al₂O₃/H₂O nanofluid in present simulation.

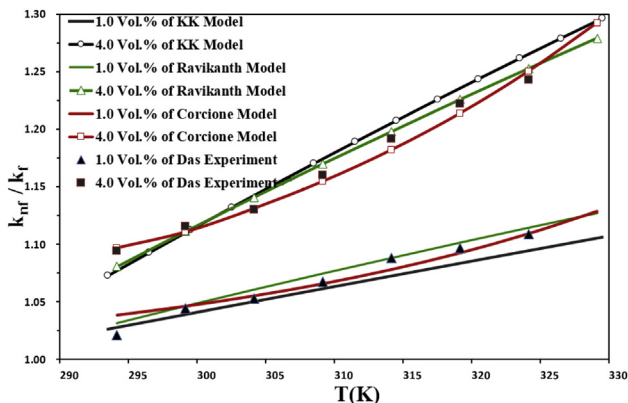


Fig. 1. Comparison of thermal conductivity of Al₂O₃/H₂O nanofluid between the predicted values using different models and experimental results.

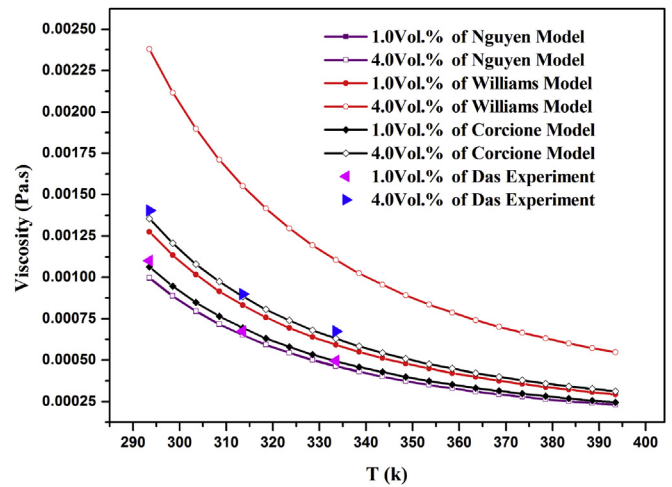


Fig. 2. Comparison of dynamic viscosity of Al₂O₃/H₂O nanofluid between the predicted values using different correlations and experimental results.

2.3. Surface tension

It is scarce that the data of nanofluids surface tension in the published papers. Zhu et al. (2010) experimental results showed that the surface tension of Al₂O₃/water nanofluids were decreased with increasing of temperature, just like that of pure water. A maximum enhancement for the surface tension of only about 5% was obtained at a concentration of 1 g/L, as the nanoparticle concentration studied in their work was very low. Syszykowski equation of Eq. (15) (Gu et al., 2004) reflects the relationship between the temperature and the surface tension of nanofluids and pure water. The experiment results from Zhu et al. (2010) are used to fit the factors of a and b as: $a = 7.673 \times 10^{-7}$, $b = -7.773 \times 10^{-3}$. Fig. 3 compares the surface tension of Al₂O₃/H₂O nanofluid between the experiment results (Das et al., 2003a, 2003b) and predicted values by Eq. (15) with fitted a and b. The deviation between the predicted values by Eq. (15) at 1.0 vol% and experiment result is less than 4.35%. Thus, Syszykowski equation (15) is supposed to be appropriate for predicting the surface tension of Al₂O₃/H₂O nanofluid.

$$\frac{\sigma_f - \sigma_{nf}}{\sigma_f} = b \ln\left(\frac{\phi}{a} + 1 \right) \tag{15}$$

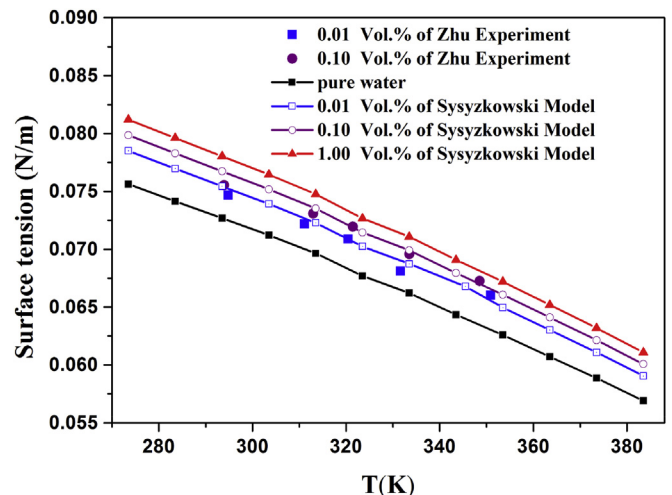


Fig. 3. Comparison of the surface tension of Al₂O₃/H₂O nanofluid between the fitted curves and experimental results.

3. Numerical simulation of bubble growth and departure during Al₂O₃/H₂O nanofluids flow boiling

3.1. Numerical method

The conventional mesh method is unqualified to simulate the interface with severe deformation. Nevertheless, Koshizuka and Oka (1996) proposed a new meshless method named the Moving Particle Semi-implicit method (MPS) which is based on Lagrangian coordinate system can catch this change accurately. However, for the flow condition with outlet and inlet, it is a large number of the particles which need to trace in Lagrangian coordinate system so that the computer capacity is much high-demanding. Thus, Yoon et al. (2001) presented an improved MPS method by introducing the method of Meshless Advection using Flow-directional Local-grid (MPS-MAFL), which is a combination of particle and meshless methods, to analyze the complex moving interface problem with inlet and outlet flow. Compared with MPS, MPS-MAFL has two more steps, one is the relocation of the particles and the other is Eulerian calculation, this makes the number of particles traced much smaller and improves the calculation efficiency. In this method, Each deferential operator appeared in the governing equation is replaced by the particle interaction model, and the weight function and models can be found in Yoon's paper. In addition, for the present work, some auxiliary models are required to be considered as follow.

3.1.1. Interface force balance model

In the field of bubble dynamic behavior, the gas pressure interior of the bubble, surface tension of the interface and the liquid pressure out of the bubble have formed a force balance system. For the condition of 3-dimension, it can be described as Eq. (16) and Fig. 4. As $d\theta$ is the equivalent infinitesimal of $d\varphi$, Eq. (16) can be simplified as Eq. (17). For the condition of 2-dimension, Eq. (16) is changed as Eq. (18), and the diagram is just like Fig. 5, as $d\varphi$ is the infinitesimal of higher order of $d\theta$, Eq. (18) can be simplified as Eq. (19).

$$P_g r^2 d\theta d\varphi - P_L r^2 d\varphi d\theta = \sigma r d\theta \sin d\theta + \sigma r d\varphi \sin d\varphi \quad (16)$$

$$P_g - P_L = \frac{2\sigma}{r} \quad (17)$$

$$P_g r d\theta - P_L r d\theta = \sigma \sin d\theta \quad (18)$$

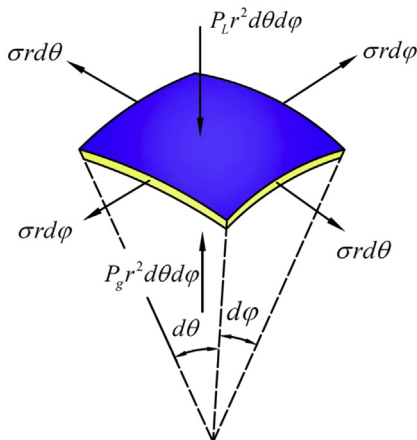


Fig. 4. 3D interface force balance model.

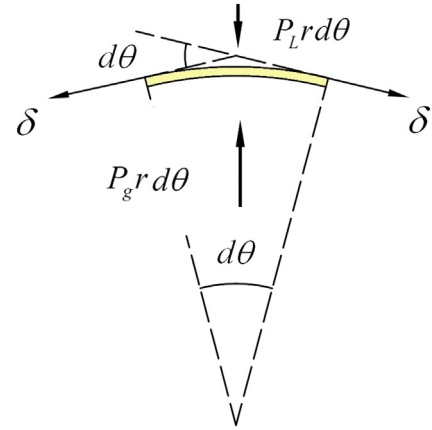


Fig. 5. 2D interface force balance model.

$$P_g - P_L = \frac{\sigma}{r} \quad (19)$$

3.1.2. Interface heat and mass transfer model

In the present work, the steam in the bubble is assumed to be saturated, so that the interface heat and mass transfer model is just shown in Fig. 6. The total phase-change heat Q is composed by Q_l (the heat from the superheat liquid, calculated by Eq. (20)) and Q_g (the heat from heating surface and transferred through the steam, calculated by Eq. (21)), and the volume changed variation in ever time layer is calculated by Eq. (23).

$$Q_l = \rho_f c_{p,f} d r^2 \sum_{i=interface} (T_i^{t+\Delta t} - T_i^t) \quad (20)$$

$$Q_g = \frac{A_g k_g (T_w - T_{Bi}) \Delta t}{\delta_g} \quad (21)$$

$$Q = Q_l + Q_g \quad (22)$$

$$\Delta V = \frac{Q}{h_{fg} \rho_g} \quad (23)$$

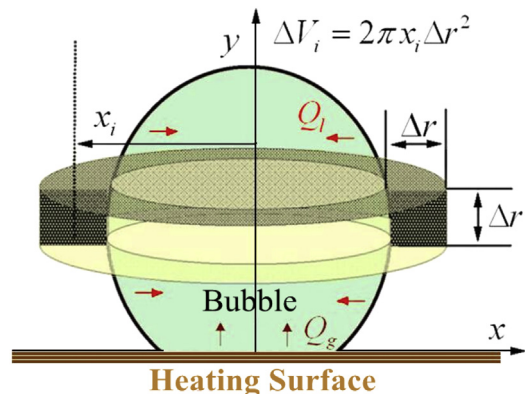


Fig. 6. Interface heat and mass transfer model.

3.2. Numerical result and discussion

3.2.1. The effect of flow boiling conditions on bubble evolution during Al₂O₃/H₂O nanofluid and pure water flow boiling

For the first step, the single bubble growth and departure is simulated in two-dimensional coordinates. The physical properties of Al₂O₃/H₂O nanofluid with volume concentration of 1.0% and nanoparticle diameter of 38 nm in 0.1 MPa pressure are shown in Table 1. In this simulation, the selected models of thermal conductivity, dynamic viscosity and surface tension of Al₂O₃/H₂O nanofluid described in section 2 are integrated into the governing equations to reflect the effects of nanoparticles volume concentration and diameter on the bubble growth and departure during flow boiling.

Just like pure fluid, except the fluid thermo-physical properties, the factors influencing the bubble growth and departure of flow boiling process include the contact angle between the bubble and the wall, the velocity of the fluid, the wall superheat and fluid subcooling. The flow boiling conditions are listed in Table 2 in which five cases are included. The bubble diameter at the moment of departure, the bubble departure frequency (reciprocal of the sum of departure time plus waiting time) and the heat flux of the heating surface of Al₂O₃/H₂O nanofluid flow boiling were investigated and compared with those of pure water under the same

conditions. For the sake of convenience of comparison, the temperature rise of all particles and the phase-change heat transfer are counted to calculate the heat flux on the heating surface in every runtime layer. The initial size of the bubble for every case is 0.4 mm. Fig. 7 shows the initial shape of the bubble and the layout of the particles. It should be noted that the star of “★” on the curves in the following figures represents the critical moment when the bubble departs from the heating surface. This moment also includes the information of the departure diameter and time (or departure frequency) of bubble. Theoretically, larger bubble departure diameter and less departure time (higher departure frequency) are benefit to boiling heat transfer.

Fig. 8 shows the changing of the bubble diameter during the flow boiling process of pure water and nanofluids under the conditions of different contact angles (case 1 and case 2), and Fig. 9 shows the bubble diameter increasing rate during the heating process. The numerical simulation results of evolution of diameter and bubble shapes in pure water for case 1 are quite clear to the experimental results of evolution of diameter and bubble shapes in pure water for case 1 (Maity, 2000), this illustrates that the results of MPS-MAFL are reliable. As shown in these two figures, the bubble grows faster and departs from the heating surface earlier as the contact angle decreasing for Al₂O₃/H₂O nanofluid as well as for pure water. Compared with pure water, the bubble departure

Table 1
Properties of water-based alumina nanofluids.

Property	Correlation	Value	Unit
Density	$\rho_{nf} = \rho_p \phi + \rho_f (1 - \phi)$	9.885×10^2	kg m ⁻³
Specific heat at constant pressure	$c_{p,nf} = \frac{(1-\phi)\rho_f c_{pf} + \phi\rho_p c_{pp}}{(1-\phi)\rho_f + \phi\rho_p}$	4.212×10^3	J kg ⁻¹ K ⁻¹
Thermal conductivity	$\frac{k_{nf}}{k_f} = 1 + 4.4Re^{0.4}Pr^{0.66} \left(\frac{T}{T_f}\right)^{10} \left(\frac{k_p}{k_f}\right)^{0.03} \phi^{0.66}$	7.841×10^{-1}	W m ⁻¹ K ⁻¹
Dynamic viscosity	$\eta_{nf} = \eta_f(T) / [1 - 34.87(d_p/d_f)^{-0.3}\phi^{1.03}]$	2.972×10^{-4}	Pa s
Surface tension	$\frac{\sigma_{f0} - \sigma_{nf}}{\sigma_{f0}} = b \ln\left(\frac{\phi}{a} - 1\right)$	6.319×10^{-2}	N m ⁻¹
Thermal diffusivity	$\alpha_{nf} = k_{nf} / (\rho_{nf} c_{p,nf})$	1.884×10^{-7}	m ² s ⁻¹
Prandtl number	$Pr_{nf} = \eta_{nf} / (\rho_{nf} \alpha_{nf})$	1.478×10^0	1

Table 2
Computational conditions.

Case	Computational condition			
	Contact angle (rad)	Wall superheat (K)	Fluid subcooling (K)	Fluid velocity (m/s)
Case 1 (standard)	$\pi/4$	5.3	0.2	0.076
Case 2 (contact angle)	$\pi/6$	5.3	0.2	0.076
Case 3 (wall superheat)	$\pi/4$	10.6	0.2	0.076
Case 4 (fluid subcooling)	$\pi/4$	5.3	1.2	0.076
Case 5 (fluid velocity)	$\pi/4$	5.3	0.2	0.115

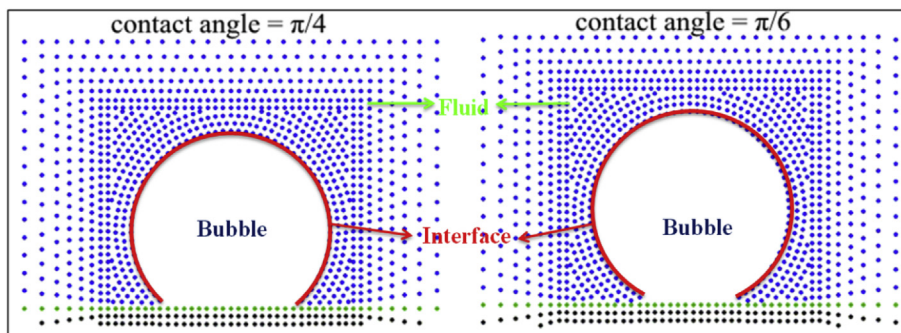


Fig. 7. The initial shape of the bubble and layout of the particles.

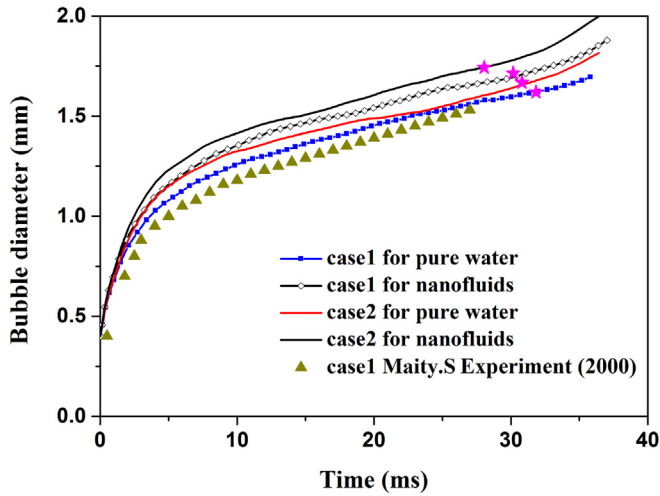


Fig. 8. Evolution of bubbles diameters of nanofluids and pure water in heating process at different contact angles.

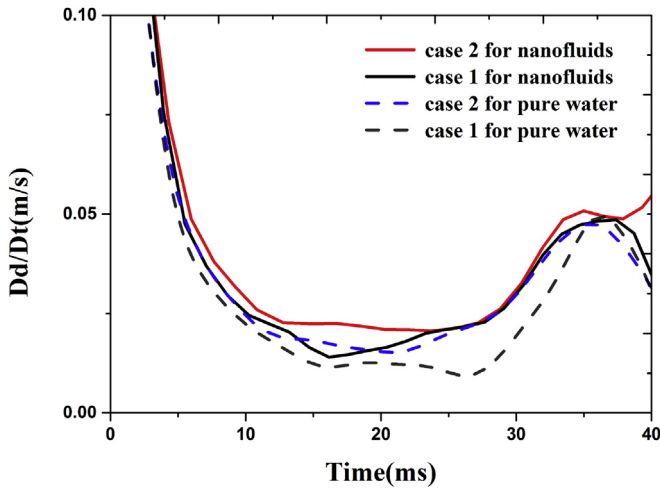


Fig. 9. Bubble diameter increasing rate during the heating process.

frequency and diameter in Al_2O_3/H_2O nanofluid are increased. This implies that the bubble takes away more heat per unit time from heating surface during flow boiling process by adding nanoparticles in pure water. For nanofluids pool boiling, Kwark et al. (2010) indicated that as vapor bubbles grow, the evaporating liquid leaves behind nanoparticles which then concentrate near the base of the bubble. A microlayer with more nanoparticles may form near the heating surface. This microlayer may benefit to decrease the contact angle between the bubble and the heating surface in nanofluids and enhance pool boiling heat transfer. This provides us an interesting clue on how to decrease the contact angle between the bubble and the heating surface, but not just improve the wettability of heating surface to enhance pool boiling heat transfer. Fig. 10 shows the evolution of the bubble shape with time for case 1 and case 2. We also find that the bubble in the nanofluid grows faster and detaches from the heating surface with larger diameter.

Fig. 11 shows the changing of the bubble diameter during the flow boiling process of pure water and Al_2O_3/H_2O nanofluid in different wall superheat conditions (case 1 and case 3). Naturally, the bubble grows faster and departs earlier in Al_2O_3/H_2O nanofluid with the increasing of the wall superheat, which is the same as that in pure water. Compared with pure water, the bubble departure

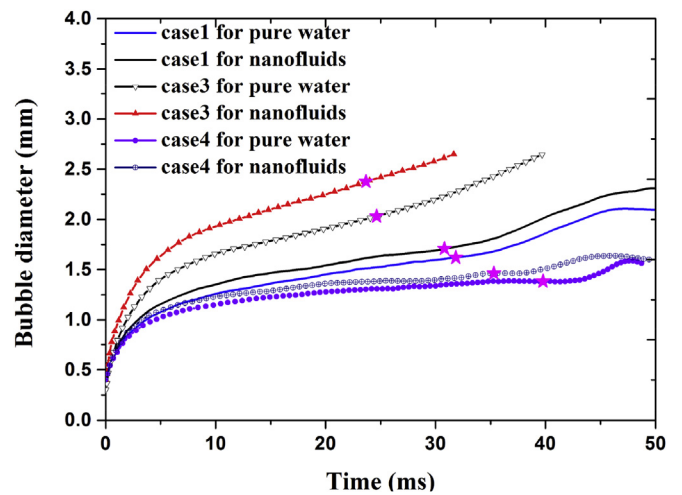


Fig. 11. Evolution of bubbles diameters of nanofluids and pure water in heating process at different degrees of wall superheat and fluid subcooling.

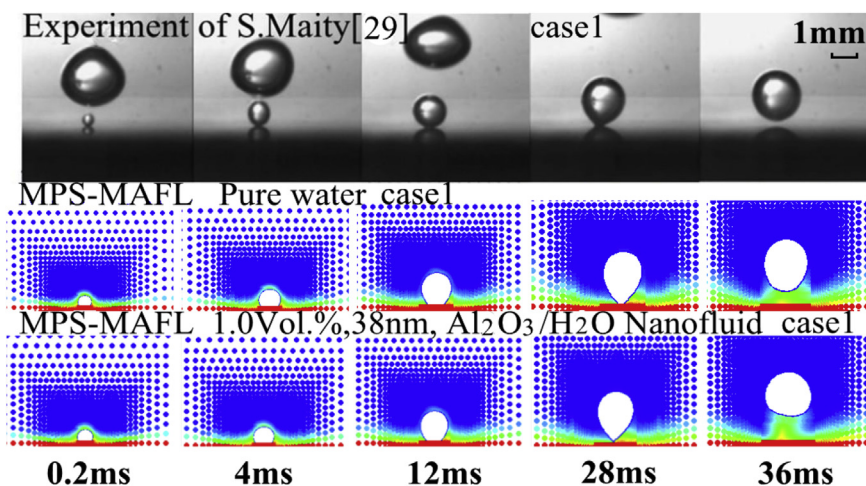


Fig. 10. Evolution of bubbles shapes of nanofluids and pure water in heating process at different contact angles.

frequency and diameter are increased by using $\text{Al}_2\text{O}_3/\text{H}_2\text{O}$ nanofluid. Meanwhile, Fig. 11 also compares that the changing of the bubble diameter during the flow boiling process of pure water and nanofluids in different fluid subcooling conditions (case 1 and case4). As shown in Fig. 11, the bubble grows more slowly and departs later in $\text{Al}_2\text{O}_3/\text{H}_2\text{O}$ nanofluid with the increasing of the fluid subcooling, which is the same as that in pure water. Again, the bubble departure frequency and diameter in $\text{Al}_2\text{O}_3/\text{H}_2\text{O}$ nanofluid are increased comparing with those in pure water at the same fluid subcooling. Fig. 12 shows the effect of flow velocity (case 1 and case 5) on the bubble evolution in $\text{Al}_2\text{O}_3/\text{H}_2\text{O}$ nanofluid and pure water boiling process. One can find that bubble departs from heating surface earlier with the increasing of flow velocity in $\text{Al}_2\text{O}_3/\text{H}_2\text{O}$ nanofluid as well as in pure water even if not so significant because of the little change in flow velocity. Again, it confirms that nanoparticles accelerate the bubble evolution in nanofluid flow boiling compared with that in base fluid flow boiling.

From Fig. 8 to Fig. 12, it can be found that the detaching bubble in $\text{Al}_2\text{O}_3/\text{H}_2\text{O}$ nanofluid can bring away more heat per unit time from the heating surface than that in pure water. It is due to two reasons: 1) detaching bubble in $\text{Al}_2\text{O}_3/\text{H}_2\text{O}$ nanofluid has larger diameter; 2) bubble in $\text{Al}_2\text{O}_3/\text{H}_2\text{O}$ nanofluid grows faster and departs earlier. To account for it, Fig. 13 shows the heat fluxes on the

heating surface in $\text{Al}_2\text{O}_3/\text{H}_2\text{O}$ nanofluid and pure water under different boiling conditions (case 1, case 3 and case 5). It is found that under the same flow boiling condition, heat flux on the heating surface in $\text{Al}_2\text{O}_3/\text{H}_2\text{O}$ nanofluid exceeds 18–34% than that in pure water.

3.2.2. The effect of nanoparticle concentration and diameter on bubble evolution during $\text{Al}_2\text{O}_3/\text{H}_2\text{O}$ nanofluids flow boiling

In the consideration of the effects of nanoparticle volume concentration and diameter on the bubble evolution in nanofluids flow boiling process, the bubble behaviors in $\text{Al}_2\text{O}_3/\text{H}_2\text{O}$ nanofluids with volume concentration of 1.0, 2.0, 3.0 and 4.0 Vol. %, and with nanoparticle diameter of 20 nm, 29 nm, 38 nm, 47 nm and 56 nm are simulated and compared in the following.

Fig. 14 shows the effects of nanoparticle volume concentration on the bubble departure time which refers to the time cost from the beginning of bubble growth to the critical moment when the bubble departs from the heating surface. The reciprocal of departure time can be taken as the bubble, the higher the departure frequency, and the more active the boiling process. It is found that the departure time decreases with the increasing of nanoparticle volume concentration of nanofluids. This means the increasing of nanoparticle volume concentration may enhance the intensity of nanofluids boiling heat transfer. It is also found that the decreasing rate of departure time is decreased with the increasing the nanoparticle volume concentration. This means the benefit of nanofluids flow boiling heat transfer enhancement by the increasing of nanoparticle volume concentration is limited. Besides, the increasing of nanoparticle volume concentration may lead to a rapid increasing of flow resistance. Fig. 15 shows the effects of nanoparticle diameter on the bubble departure time. It is interesting to find that the departure time are decreased firstly and then increased with the increasing of the nanoparticle diameter. In the same nanoparticle volume concentration condition, the bubble departure time for the nanofluid with nanoparticle diameter of 29 nm shows a minimum value. This is due to the complicated relationship between the thermo-physical properties and nanoparticle diameter of nanofluid.

Fig. 16 shows the effects of nanoparticle volume concentration and diameter on the bubble departure diameter. Fig. 17 shows the bubble diameter changing rate at departure point for different nanoparticle volume concentration and diameter. It is found that

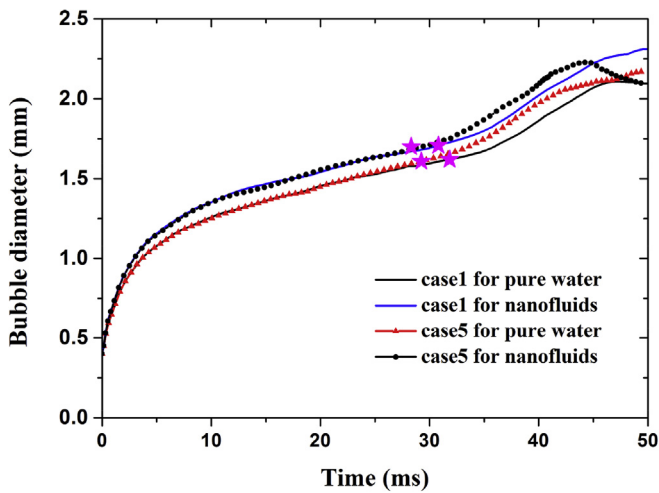


Fig. 12. Evolution of bubbles diameters of nanofluids and pure water in heating process at different flow velocities.

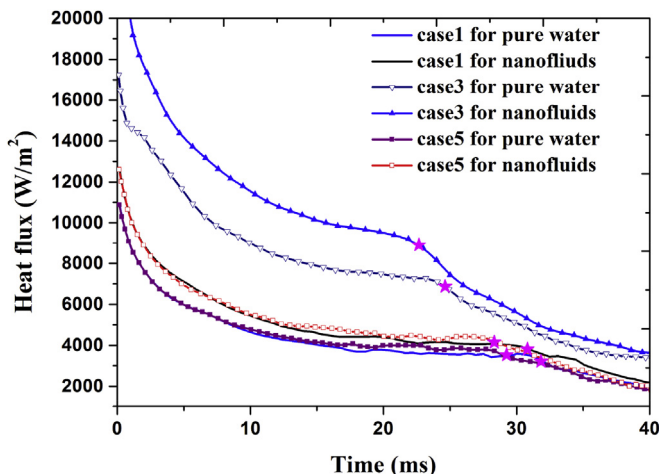


Fig. 13. Comparison of heat fluxes of pure water and nanofluids in different conditions.

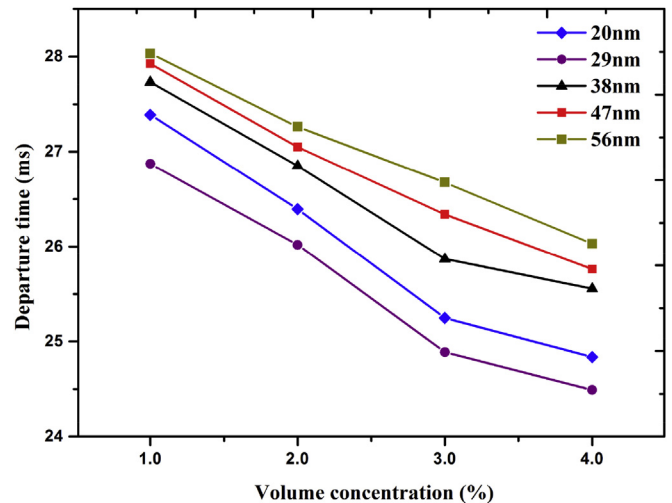


Fig. 14. Effects of nanoparticle volume concentration of nanofluid on the bubble departure time.

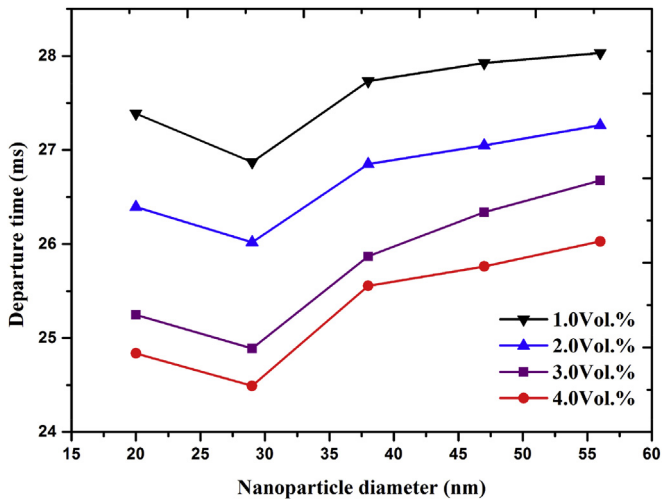


Fig. 15. Effects of nanoparticle diameter of nanofluid on the bubble departure time.

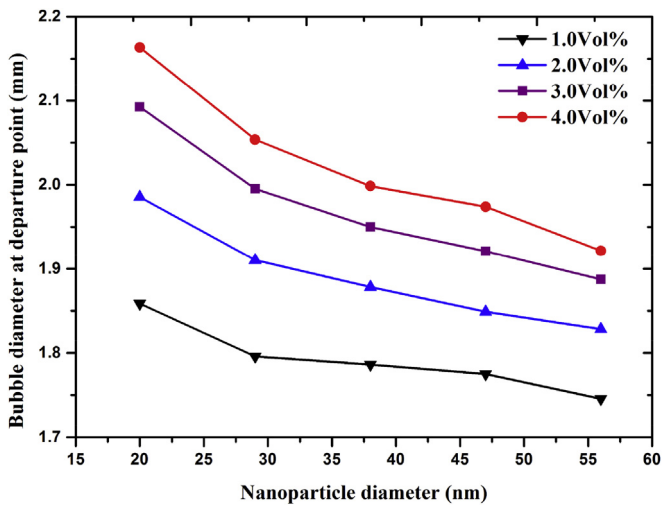


Fig. 16. Effects of nanoparticle diameter and volume concentration of nanofluid on the bubble departure diameter.

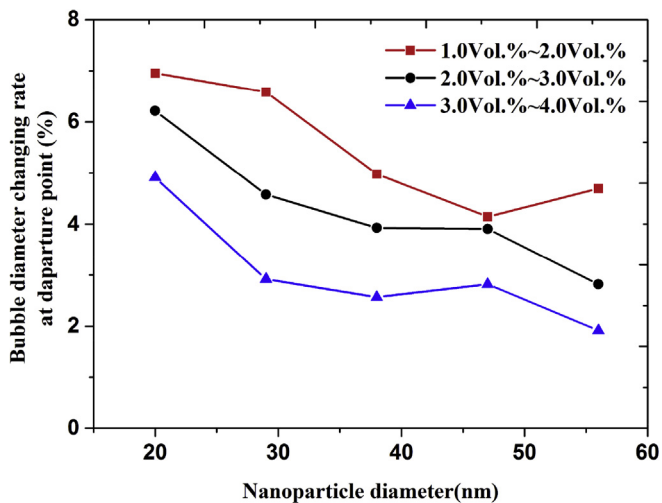


Fig. 17. Bubble diameter changing rate at departure point for different nanoparticle volume concentration and diameter.

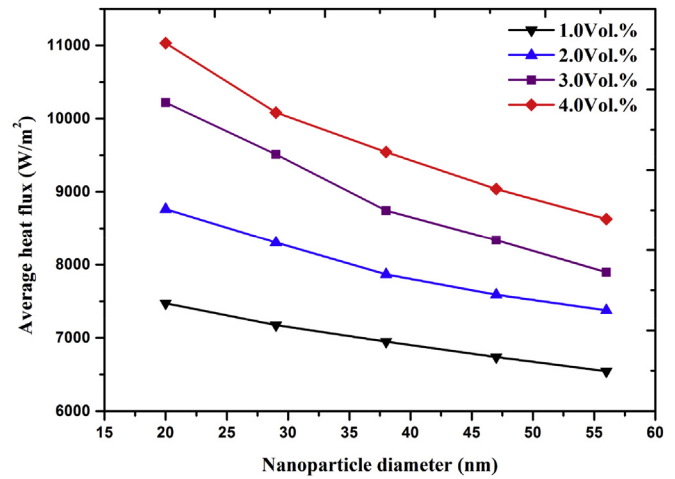


Fig. 18. Effects of nanoparticle diameter and volume concentration on the average heat flux during the heating process.

the increasing of nanoparticle volume concentration brings about the increasing of bubble departure diameter. While the increasing rate of departure diameter is decreased with the increasing of nanoparticle volume concentration. The collective effects of nanoparticle volume concentration on the bubble departure time, diameter and flow resistance indicate that the suitable nanoparticle volume concentration of nanofluid for flow boiling heat transfer enhancement should not be too high. In addition, it is found that the increasing of nanoparticle diameter leads to the decreasing of bubble departure diameter, and the decreasing rate of bubble departure diameter is reduced with the increasing of nanoparticle diameter. Combining this result with the minimum value of departure time in nanoparticle diameter of 29 nm, it is boldly predicted that an optimal nanoparticle diameter range between 20 nm and 38 nm should be beneficial to flow boiling heat transfer enhancement of Al₂O₃/H₂O nanofluid.

Fig. 18 shows the effects of nanoparticle volume concentration and diameter of Al₂O₃/H₂O nanofluids on the averaged heat fluxes on the heating surface which are counted from the beginning of bubble growth to the critical moment when the bubble departs from the heating surface. The average heat flux is decreased with increasing the nanoparticle diameter, increased with increasing the nanoparticle volume concentration. This is coincident with the result about the variation of bubble departure diameter vs. nanoparticle volume concentration and diameter of Al₂O₃/H₂O nanofluids.

4. Conclusion

In the present study, regression analysis on Al₂O₃/H₂O nanofluid's thermo-physical properties was made firstly. A single bubble's dynamics behavior of Al₂O₃/H₂O nanofluid flow boiling is then simulated by MPS-MAFL method. The key remarks of the present work are as follows:

- (1) Very small amount of solid guest nanoparticles were found to provide dramatic improvements in thermal properties of nanofluids compared with those of base fluids. Nanofluids are thus being considered as innovative and potential working fluids for heat management systems with high heat flux. Nanofluids flow boiling heat transfer characteristics is one of hot research topic in heat transfer enhancement research field.

- (2) In the same flow conditions, addition of Al_2O_3 nanoparticles may increase the bubble departure frequency and diameter in $\text{Al}_2\text{O}_3/\text{H}_2\text{O}$ nanofluid flow boiling compared those in pure water flow boiling. The bubble in $\text{Al}_2\text{O}_3/\text{H}_2\text{O}$ nanofluid may take away more heat per unit time from heating surface during flow boiling process. The present work initially reveals that nanofluids can enhance flow boiling heat transfer from the point of view of bubble dynamics behavior.
- (3) Just like pure water, the bubble growth and departure frequency in nanofluid flow boiling are relevant to the contact angle between the bubble and the wall, wall superheat, fluid subcooling and the flow velocity of the fluid. The bubble departure diameter, departure frequency and the heat flux of the heating surface is increased with the decreasing of the contact angle and fluid subcooling, with the increasing of the wall superheat and flow velocity.
- (4) The diameter and the volume concentration of nanoparticle are two important factors influencing the thermo-physical properties of nanofluids, Thus bubble behavior in nanofluid flow boiling should be affected by the diameter and the volume concentration of nanoparticle. The following findings are reached. (I) The increasing of nanoparticle volume concentration may increase the bubble departure frequency and departure diameter. (II) The increasing rates of departure frequency and departure diameter are lessened with the increasing of nanoparticle volume concentration. It is suggested that the suitable nanoparticle volume concentration of nanofluid for flow boiling heat transfer enhancement should not be too large, especially regarding the negative effect of flow resistance increase by the increasing of nanoparticle volume concentration. (III) It is interesting to find that in the same nanoparticle volume concentration condition, the bubble departure time for the nanofluid with nanoparticle diameter of 29 nm shows a minimum value. The increasing of nanoparticle diameter leads to the decreasing of bubble departure diameter. It is boldly to predict that an optimal nanoparticle diameter range between 20 and 38 nm should be beneficial to flow boiling heat transfer enhancement of $\text{Al}_2\text{O}_3/\text{H}_2\text{O}$ nanofluids.

Future work

Single bubble simulation is just the first step to study the nanofluids flow boiling characteristics. For better predict the boiling heat transfer and critical heat flux of nanofluids, the future work will focus on the other phenomena in nanofluids flow boiling process such as multi-bubbles interaction and coalescence, bubble shriveling and breakup, etc.

Acknowledgments

The present work is supported by the National Natural Science Foundation of China (No. 51276164) and the Open Fund Program of Key Laboratory of Advanced Reactor Engineering and Safety, Ministry of Education of China.

References

- Ahn, H.S., Kim, M.H., 2012. A review on critical heat flux enhancement with nanofluids and surface modification. *J. Heat. Transf.* 134 (2), 024001.1–024001.13.
- Ahn, H.S., Kim, H., Jo, H.J., Kang, S.H., Chang, W.P., Kim, M.H., 2010. Experimental study of critical heat flux enhancement during forced convective flow boiling of nanofluid on a short heated surface. *Int. J. Multiph. Flow.* 36 (5), 375–384.
- Choi, S.U.S., 1995. Enhancing thermal conductivity of fluids with nanoparticles. *ASME-Publ.-Fed* 231, 99–106.
- Corcione, M., 2011. Empirical correlating equations for predicting the effective thermal conductivity and dynamic viscosity of nanofluids. *Energ. Conv. Manage* 52 (1), 789–793.
- Das, S.K., Putra, N., Roetzel, W., 2003a. Pool boiling characteristics of nano-fluids. *Int. J. Heat. Mass Transf.* 46 (5), 851–862.
- Das, S.K., Putra, N., Thiesen, P., Roetzel, W., 2003b. Temperature dependence of thermal conductivity enhancement of nanofluids. *ASME J. Heat. Transf.* 125, 567–574.
- Einstein, A., 1956. *Investigation on the Theory of Brownian Movement*. Dover Publications, New York.
- Gu, T.R., Zhu, B.Y., Li, W.L., 2004. *Surface Chemistry*. Beijing Science Press.
- Heris, S.Z., 2011. Experimental investigation of pool boiling characteristics of low concentrated CuO/ethylene glycol water nanofluids. *Int. Commun. Heat. Mass Trans.* 38 (10), 1470–1473.
- Kim, S.J., McKrell, T., Buongiorno, J., Hu, L.W., 2008. Alumina nanoparticles enhance the flow boiling critical heat flux of water at low pressure. *Int. J. Heat. Transf.* 130 (4), 1044–1050.
- Kim, T.I., Jeong, Y.H., Chang, S.H., 2010. An experimental study on CHF enhancement in flow boiling using Al_2O_3 nano-fluid. *Int. J. Heat. Mass Transf.* 53 (5), 1015–1022.
- Kim, T.I., Chang, W.J., Chang, S.H., 2011. Flow boiling CHF enhancement using Al_2O_3 nanofluid and an Al_2O_3 nanoparticle deposited tube. *Int. J. Heat Mass Transf.* 54 (9), 2021–2025.
- Koo, J., Kleinstreuer, C., 2004. A new thermal conductivity model for nanofluids. *J. Nanopart. Res.* 6 (6), 577–588.
- Koshizuka, S., Oka, Y., 1996. Moving-particle semi-implicit method for fragmentation of incompressible fluid. *Nucl. Sci. Eng.* 123 (3), 421–434.
- Kwark, S.M., Kumar, R., Moreno, G., 2010. Pool boiling characteristics of low concentration nanofluids. *Int. J. Heat. Mass Transf.* 53 (5), 972–981.
- Maity, S., 2000. *Effect of Velocity and Gravity on Bubble Dynamics*. MS thesis. University of California, Los Angeles.
- Nguyen, C.T., Desgranges, F., Roy, G., Galanis, N., Maré, T., Boucher, S., Mintsa, H.A., 2007. Temperature and particle-size dependent viscosity data for water-based nanofluids—Hysteresis phenomenon. *Int. J. Heat. Fluid Flow.* 28 (6), 1492–1506.
- Park, K.J., Jung, D., Shim, S.E., 2009. Nucleate boiling heat transfer in aqueous solutions with carbon nanotubes up to critical heat fluxes. *Int. J. Multiph. Flow.* 35 (6), 525–532.
- Taylor, R.A., Phelan, P.E., 2009. Pool boiling of nanofluids: comprehensive review of existing data and limited new data. *Int. J. Heat. Mass Transf.* 52 (53), 5339–5347.
- Truong, B.H., 2007. Determination of pool boiling critical heat flux enhancement in nanofluids. In: *ASME 2007 International Mechanical Engineering Congress and Exposition*. ASME, pp. 289–299.
- Vafaei, S., Wen, D.S., 2011. Flow boiling heat transfer of alumina nanofluids in single microchannels and the roles of nanoparticles. *J. Nanopart. Res.* 13 (3), 1063–1073.
- Vajjha, S.R., Das, D.K., 2009. Experimental determination of thermal conductivity of three nanofluids and development of new correlations. *Int. J. Heat. Mass Transf.* 52 (21), 4675–4682.
- Williams, W., Buongiorno, J., Hu, L.W., 2008. Experimental investigation of turbulent convective heat transfer and pressure loss of alumina/water and zirconia/water nanoparticle colloids (nanofluids) in horizontal tubes. *J. Heat. Transf.* 130 (4), 040301.1–044503.4.
- Xu, L., Xu, J.L., 2012. Nanofluid stabilizes and enhances convective boiling heat transfer in a single microchannel. *Int. J. Heat. Mass Transf.* 55 (21), 5673–5686.
- Yoon, H.Y., Koshizuka, S., Oka, Y., 2001. Direct calculation of bubble growth, departure, and rise in nucleate pool boiling. *Int. J. Multiph. Flow.* 27 (2), 277–298.
- You, S.M., Kim, J.H., Kim, K.H., 2003. Effect of nanoparticles on critical heat flux of water in pool boiling heat transfer. *Appl. Phys. Lett.* 83 (16), 3374–3376.
- Zhu, D.S., Wu, S.Y., Wang, N., 2010. Surface tension and viscosity of aluminum oxide nanofluids. *AIP Conf. Proc.* 1207, 460–464.